Effect of Anion-exchange Membrane Surface Properties on Mechanisms of Overlimiting Mass Transfer

Elena I. Belova,[†] Galina Yu. Lopatkova,[†] Natalia D. Pismenskaya,[†] Victor V. Nikonenko,*[,†] Christian Larchet,[‡] and Gerald Pourcelly[§]

Physical Chemistry Department, Kuban State University, 149 Stavropolskaya str., 350040 Krasnodar, Russia, Laboratoire Matériaux Echangeurs d'Ions, Université Paris XII, av. du Général de Gaulle, 94010 Créteil Cedex, France, and Institut Européen des Membranes, Université Montpellier II, Place Eugène Bataillon, 34095 Montpellier Cédex 5, France

Received: April 20, 2006; In Final Form: May 19, 2006

Four effects providing overlimiting current transfer in ion-exchange membrane systems are examined. Two of them are related to water splitting: the appearance of additional current carriers (H^+ and OH^- ions) and exaltation effect. Two others are due to coupled convection partially destroying the diffusion boundary layer: gravitational convection and electroconvection. Three anion-exchange membranes, which differ in surface morphology and the nature of ion-exchange sites within a surface layer, are examined. The ion transfer across these membranes in NaCl solutions is studied by voltammetry, chronopotentiometry, and pH-metry. By excluding the effects of water splitting and gravitational convection, it is shown that the main mechanism of overlimiting mass transfer in narrow membrane cells at low salt concentrations is electroconvection. The reasons explaining why water splitting suppresses electroconvection are discussed. The scenario of development of potential oscillations with growing current and time is compared with that described theoretically by Rubinstein and Zaltzman.

Introduction

It is well-known that under a direct electric current passing through an ion-exchange membrane, concentration gradients develop in electrolyte solution adjacent to the membrane due to difference in ion transport numbers within the membrane and solution.[1] A similar phenomenon takes place in electrode systems. Following the classical electrochemical interpretation, the formation of concentration gradients results in saturation of the current density (i) caused by the vanishing interface concentration; when i tends to its limiting value (i_{lim}), the potential drop over the system tends to infinity. However, in real membrane and electrode systems, the limiting current density can be exceeded by several times. A complex of effects related to the formation of current-induced concentration gradients (named "concentration polarization",[2] in the general sense of the term) occurs near the membrane (electrode) surface, accounting for, in particular, the overlimiting current phenomenon. The understanding of mechanisms responsible for overlimiting current transfer is important for improving electrodialysis and electrodeionization. Besides, as coupled convection is involved in these mechanisms, their study is of interest for electrokinetic micropumps[3], electrophoresis,[4,5] electrodeposition,[6] and layering of colloid crystals on electrode surfaces.[7]

Actually, in the literature, four effects explaining the overlimiting transfer are discussed. The two first are related to the water splitting at the membrane/solution interface. The water splitting in membrane systems was observed by numerous researchers,[8−11] and for a long time, the transfer of current by additional carriers, H^+ and OH^- ions, was considered as the main and often the sole reason for the overlimiting conductance.[12] The generation of H^+ and OH^- ions causes another, less evident, mechanism of overlimiting transfer, the exaltation effect, first studied by Kharkats.[13] The emergence of H^+ and OH^- ions near the interface disturbs the electric field that can increase (exalt) the salt counterion transfer: for example, the OH^- ions generated into the depleted diffusion layer at a cation-exchange membrane attract the salt cations from the solution bulk toward the interface. The flux density of salt counterions (j_1) is described by the following equation[13]

$$j_1 = \frac{2D_1c^0}{\delta} + \frac{D_1}{D_w}j_w \qquad (1)$$

where D_1 and c^0 are the diffusion coefficient and bulk concentration of the salt counterion, δ is the diffusion layer thickness, and D_w and j_w are the diffusion coefficient and the flux density of the product of water splitting generated into the depleted diffusion layer, the OH^- ion in the case of the cation-exchange membrane. As can be seen from Kharkats' eq 1, the augmentation of salt counterion flux beyond its limiting value is proportional to the flux of generated OH^- (H^+) ions, the coefficient of proportionality is equal to D_1/D_w. The increment in salt counterion flux due to the exaltation effect is not too high: it is equal approximately to $0.2i_{lim}$ when the flux of the OH^- ion reaches i_{lim}. In practice, the increment of salt counterion flux is noticeably higher;[14,15] hence, this cannot be explained by the exaltation effect. Thus, two other mechanisms of overlimiting transfer should contribute essentially. These are two types of coupled convection providing additional, in comparison with forced convection, mixing of depleted solution. This mixing is produced by local vortices resulting from the action of current-induced volume forces.

* To whom correspondence should be addressed. E-mail: v_nikonenko@mail.ru. Tel/fax: +7 861 219 95 73.
[†] Kuban State University.
[‡] Université Paris XII.
[§] Université Montpellier II.

10.1021/jp062433f CCC: $33.50
Published on Web 06/20/2006

The first type of coupled convection is gravitational convection, which arises due to the nonuniform distribution of solution density; the latter causes Archimedean volume force bringing the liquid in motion.[16−18] The second type is electroconvection occurring due to the action of the electric field on the electric space charge in the boundary depleted solution.[2,19−21]

In the case of gravitational convection, the rise of volume force is conditioned by gradients of concentration and/or temperature.[16−18] Hence, this phenomenon is more likely to occur in relatively concentrated solutions because of higher Joule heating (caused by higher current density under the same voltage) and higher concentration gradients.[22,23] In membrane systems, it was established experimentally[15,22] that the contribution of the gravitational convection in overlimiting current transfer is negligible in the case of narrow intermembrane spacing (h) and small solution concentration (c^0), whereas the solution flow velocity (V) is high. In experiments,[15,22] this contribution was negligible when $h = 1$ mm, $c^0 < 0.02$ M NaCl, and $V > 0.07$ cm s^{-1}. In the general case, it is known[17] that, when the solution/permselective solid interface (with an electrode or a membrane) is vertical and the density gradient is horizontal, the gravitational convection arises without threshold. When the interface is situated horizontally, more precisely, when the density of a solution situated between two parallel horizontal plates varies progressively along with the normal coordinate, two cases are possible. If the lighter solution layer (normally, the depleted layer) is on the top of solution layer, then no convection arises. If the lighter layer is at the bottom, then there is a threshold in development of the gravitational convection determined by the Rayleigh number[16−18]

$$Ra = \frac{\Delta\rho}{\rho}\frac{gd^3}{\nu D} \qquad (2)$$

where $\Delta\rho$ is the variation in the solution density (ρ) between the top and bottom, d is the characteristic distance within which the density varies, g is the free-fall acceleration, ν is the viscosity, and D is the electrolyte diffusion coefficient. The system is stable if $Ra < Ra_{cr} = 1708$: the characteristic time, which is necessary for diffusion relaxation of a density fluctuation in a small solution volume, is less than the characteristic time of heaving of this volume. If $Ra > Ra_{cr}$, then the volume with negative fluctuation in density lifts with acceleration, as the density within the volume increases more slowly, when the volume lifts, than the density in the environmental solution. The amplitude of small perturbations in this case increases with time, and the solution between the plates reaches a state with a periodic cellular vortex structure where the liquid within two neighboring cells (the Bénard cells) rotates in opposite directions.[17,18,24] A theoretical study of gravitational convection in electrochemical systems was undertaken in refs 5, 18, 24, and 25. The review of works devoted to the problem of hydrodynamic instability of gravitational convection is made by Volgin and Davydov.[18] Experimentally, the gravitational convection in electrochemical systems was studied in refs 15, 22, and 26−31. The contribution of gravitational convection into the mass transfer was evaluated by voltammetry;[22] its influence on the concentration polarization of membrane system was examined by chronopotentiometry.[31] The convection motion was visualized in[26,27] by using laser interferometry. The cellular structure was studied by using a combination of optical methods and chronopotentiometry,[28,29] as well by wavelet and Fourier analysis of noise spectrum.[28,30] In particular, the development of vortices with time is described in a horizontal membrane system; it was found that the onset of current-induced gravitational convection corresponds to the frequency of vortex rotation in the range of 0.1−0.4 s^{-1}.[30] Vessler et al.[29] have established experimentally that the onset of coupled convection in electrochemical systems can be at $Ra < Ra_{cr} = 1708$, which is explained by the action of Coulombic forces, that is, by electroconvection.

Rubinstein et al.[2,32−34] have theoretically analyzed two principle modes of electroconvection: "bulk" electroconvection, which is due to the volume electric forces acting on a macroscopic scale in a locally quasielectroneutral electrolyte, and electroosmosis, either of the classical "first" kind or of the "second" kind, according to terminology proposed by Dukhin and Mishchuk.[19−21] It was shown[33] that the hydrodynamic instability of the membrane system cannot be originated from the bulk electroconvection. Electroosmosis of the "first" kind occurs as the electrolyte slip caused by the action of the tangential electric field upon the space charge of a quasi-equilibrium electric double layer.[2,19−21,32−34] The most probable mechanism of intensive electroconvective mixing and electrochemical noise observed in ion-exchange membrane systems at overlimiting currents is electroosmosis of the second kind first studied by Dukhin and Mishchuk.[19−21] The electroosmosis of the second kind is similar to that of the first kind with the difference that the electric field acts upon the extended space charge region (SCR) induced by the same electric field,[2,19−21,35] which can be considered as a nonequilibrium double layer occupying a region several orders of magnitude larger than the equilibrium one.[2,21,36] Note that the applied electric force should not be necessarily tangential. When an electric force directed normally to the membrane acts on the space charge localized near the interface, an excess pressure arises within the SCR. This excess pressure displaces the liquid out from the SCR in tangential direction. When moving, the displaced liquid meets inertial resistance of nonslipping liquid layers that changes the direction of moving liquid toward the solution bulk. As a result, a pair of vortices rotating in opposite senses appears, if the system is considered as two-dimensional.[2,15] This convection causes mixing of the depleted solution near the interface that can be also interpreted as partial destruction of the diffusion boundary layer (DBL) resulting in an increase in the limiting current density.

If a charge is uniformly distributed in space and is exposed to a uniform electric current, then the electric force applied is the same at any point, which cannot cause moving of a part of quiescent fluid when the other part remains still. However, even near a perfectly flat homogeneous membrane, the space charge cannot stay ideally quiescent and uniform. First, it is always nonuniform along the normal distance from the membrane. Second, nonuniformities may arise spontaneously as a result of fluctuation of current in time or space. Rubinstein and Zaltzman[2] have shown that a nonequilibrium electroosmotic slip at a homogeneous permselective membrane (electroosmosis of the second kind) yields instability of the quiescent concentration polarization.[2,32−34] However, the presence of electrical nonuniformity on the membrane surface, under the form of a nonflat surface or alternate well and less well-conducting regions, should facilitate the rising of electroconvection.[2,15,21,23,35] The situation may be compared with that occurring in hydrodynamics where the passage from a laminar to turbulent regime of a fluid flowing within a channel is facilitated by the presence of obstacles. Rubinstein and Zaltzman[2] have theoretically studied the electroosmotically induced convection near a membrane with waved surface. The case of a spherical surface of an ion-exchange resin granule is considered theoretically by Mishchuk and Dukhin;[19−21] the role of surface shape in developing electroconvection in ion-

exchange systems was studied theoretically and experimentally by Mishchuk, Gonzales-Caballero, and Takhistov.[35] Evidently, a nonuniform distribution of SCR takes place near a heterogeneous membrane.[2,21,23]

The rate of electroconvection should depend not only on the space charge and applied electric force values but also on the Stokesian radius of ions forming the SCR as well. Indeed, the more this radius is great, the more effective the liquid is involved in motion.

Choi et al.[37] has drawn attention to this circumstance and studied the membrane behavior in different electrolyte solutions. Effectively, they have found that the relative increment in overlimiting current, which should be apparently related to the electroconvection, increases with the Stokesian radius.

The heterogeneity of the membrane surface conditions the presence on the surface of regions of different conductance that results in opposite, regarding the transfer rate, effects. On one hand, this heterogeneity gives rise to nonuniformity in SCR distribution and facilitates the initiation of vortices generation.[2,21,23] In the case of the waved surface, the voltage threshold, upon which the overlimiting conductance starts, is noticeably less than that for a flat membrane;[2,21,32] a 10% distortion of the flat membrane surface results in a 30% increase in the current.[2] On the other hand, in the case of the heterogeneous surface, the current lines are distributed nonuniformly over the membrane surface: they are concentrated in the regions with good conductivity. As a consequence, the local current density through these regions is higher, in comparison with the case of a homogeneous interface and the same average current density. Hence, if the DBL thickness is the same in two systems under comparison, then the concentration polarization of the heterogeneous membrane is higher: the interface concentration near the conductive regions is lower and the potential drop is greater.[38−40] The gain in the mass transfer rate in a heterogeneous membrane system may be in the case where the factor of reducing the DBL thickness by more intensive coupled convection is dominant. Theoretically, it is possible; this gain is experimentally established for waved membranes or the membranes with a relief profiled surface.[41−43] One of the effects of a nonflat surface consists according to theory[2] in decreasing the voltage value at which the electroconvection becomes effective and gives significant rise to the overlimiting current. When measuring the current−voltage curves, this is expressed in the diminishing length of the plateau of the limiting current. Ibanez, Stamatialis, and Wessling[44] have reported about preliminary experiments with cation-exchange membranes having undulated surface showing a decrease in the plateau length while the limiting current remains the same as that for the origin flat membrane. However, we do not know direct observations in which, under the same conditions, the mass transfer rate was higher through a flat heterogeneous membrane than through a homogeneous one, in usual strong electrolyte solutions.

The role of surface morphology in the overlimiting transfer was studied in a number of papers.[38−40,45−47] Balavadze, Bobreshova, and Kulintsov[45] have found that the average limiting current density is higher through a homogeneous cation-exchange membrane (an experimental perfluorinated sulfocationic PSM membrane) in comparison with heterogeneous ones (such as MK-40), under the same hydrodynamic conditions. Similar results were obtained by Vyas et al.[46] and in our papers:[40,47] under the same current density, the potential drop across heterogeneous membranes is higher in comparison with homogeneous membranes including the case where the current density exceeded its limiting value. The works of Berezina et al.[48,49] merit attention because higher current density, in overlimiting current regimes, under the same voltage was observed through a heterogeneous MK-40 membrane and a homogeneous MF-4SK membrane after inducing in the solution a small quantity of some surfactant, for example, camphor. Measurements with laser interferometry have shown that adding such surfactants results in a decrease in the DBL thickness and an increase in oscillations of interferograms at overlimiting currents. The authors[49] explain these effects by the rise of hydrodynamic flows within the solution DBL under the action of local electric and surface forces.

The aim of this paper is to give a new insight in establishing mechanisms controlling the overlimiting mass transfer under different conditions and in elucidating how experimental observations correlate with known theoretical studies. We will consider the electrochemical behavior of homogeneous and heterogeneous membranes under conditions favorable and not favorable for gravitational convection. In particular, the behavior of two membranes with the same surface morphology but with different ability to split water will be compared.

Experimental Section

Materials. Three anion-exchange membranes are studied. The first one is a commercial homogeneous AMX membrane manufactured by Tokuyama Soda, Japan; the second one is a commercial heterogeneous MA-40 membrane manufactured by NPO "Schekinoazot", Russia, and the third one (MA-40-13) is an experimental MA-40 membrane specially treated by NPO "Vladipor", Russia, to reduce its ability to split water at overlimiting currents.

According to the manufacturer,[50] the homogeneous AMX membrane contains fixed quaternary ammonium groups. Even the catalytic activity of these groups in regard to water splitting is low,[9] the AMX membrane is known as a membrane able to split water with a moderate rate at overlimiting currents. The surface of this membrane is rather homogeneous and smooth; the size of small nonuniformities seen on the surface (Figure 1a) (perhaps, bacteria or motes) is of the order of 1 μm.

The heterogeneous MA-40 membrane contains fixed tertiary and secondary amine fixed groups,[51] which provide a high water splitting rate.[9] The MA-40-13 membrane is a sample of MA-40 membrane treated by a polyelectrolyte complex; as a result, the tertiary and secondary amine groups within a surface layer of about 80 μm in thickness are converted into quaternary amino groups. The MA-40 and MA-40-13 membranes are characterized by the same surface morphology: most of the surface is covered by polyethylene, which is used as a filling fastening together small (about 30 μm in diameter) particles of anion-exchange resin; the active surface forming 21% of total surface is constituted by ion-exchange particles projecting from the polyethylene layer (parts b and c of Figure 1). As we will see below, the rate of water splitting is considerably lower for the MA-40-13 membrane.

The main characteristics of studied membranes are presented in Table 1.

The experiments were performed with NaCl solutions of two concentrations, 0.005 and 0.1 M. The first concentration was chosen for decreasing the solution density drop in the measuring cell to eliminate the gravitational convection.

Membrane Surface Study. An electronic scanning microscope LEO (ex LEICA, ex CAMBRIDGE) Type S260 was used to obtain the microphotographs of the membrane surface and cross-sections. Before taking the photographs, the membranes

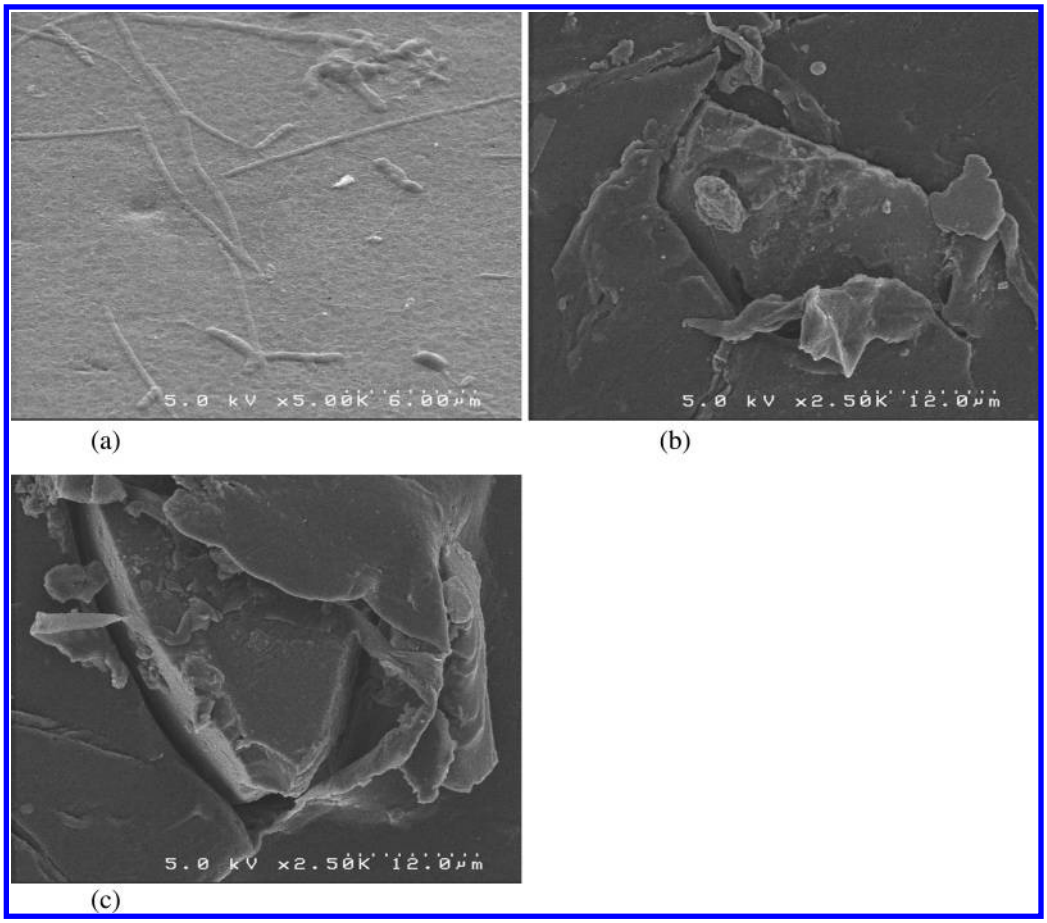

Figure 1. Microphotographs of the membrane surface: (a) AMX, (b) MA-40, and (c) MA-40-13.

TABLE 1: Main Characteristics of Investigated Membranes

membrane	AMX	MA-40	MA-40-13
ionogenic groups	$-N(CH_3)_3^+$	$=NH$, $\equiv N$	$-N(CH_3)_3^+$, $=NH$, $-NH_2$, $\equiv N$
inert binder		polyethylene	polyethylene
exchange capacity[a], meq g^{-1}	1.55 ± 0.15	2.94 ± 0.10	2.90 ± 0.10
Cl^--form of wet membrane			
water content, $g_{H_2O}\, g^{-1}$	0.25−0.30	0.35−0.45	
Cl^--form of dry membrane			
thickness[a], μm	130 ± 10	460 ± 20	480 ± 20
κ[a], mSm cm^{-1} in 0.1 M NaCl	6.0	3.2	5.0
κ[a], mSm cm^{-1} in 0.1 M NaOH	16.0	1.0	1.1

[a] Our data. The other data are taken from the catalogues.[50,51]

were dried at a temperature of about 35 °C to remove the humidity. The dissection of the membrane was made after dipping the sample into liquid nitrogen. Then a thin layer of platinum was sprayed onto the membrane surface.

Membrane Electrochemical Behavior Study. Current−voltage characteristics (CVC), chronopotentiometric (ChP) curves, and pH variation vs potential drop across the membrane are obtained for all studied membranes with the help of a setup described in ref 40.

The diagram of the measuring cell is represented in Figure 2. The compartments are formed by membranes (1) as well as by plastic (2) and elastic (3,4) gaskets with a square aperture of 2×2 cm^2 (5). The thickness of the plastic gaskets is 5 mm. The thicknesses of elastic gaskets (3) and (4) are 0.5 and 0.95 mm, respectively. Hence, the distance between the neighboring membranes (h) is about 7.0 mm. The compartments adjoining the membrane under study (A*) are separated from the electrode compartments by a cation-exchange membrane (C) from the side of a platinum plane cathode (6) and by an anion-exchange membrane (A) from the side of a platinum plane anode (7). Two plastic capillaries (8) are used for the sampling of solution from the layers adjoining the studied membrane from both its sides. The tips of the capillaries with an external diameter of 0.8 mm are placed at the center of the membrane at an angle of 45°; their cross-sectional plane is made to be parallel to the membrane surface and fixed at a distance of about 1 mm from it. The pH measurements of the solution flowing out from the capillaries were carried out. The flow rate of this solution did not exceed 5% of the solution flow rate through the desalination and concentration compartments, in order not to disturb the velocity distribution established by forced and natural convection. Two silver wires (Goodfellow, England) (9) with diameter 0.25 mm coated by polytetrafluorethylene with a thickness of 0.024 mm are clamped between gaskets (3) and (4) from the both sides of the membrane. The tips of the Ag wires are coated with AgCl by polarizing them as the cathode during 1 h in 0.1 M HCl solution under a direct current of 0.1 mA. These silver−silver chloride electrodes (9) are used for measuring the potential

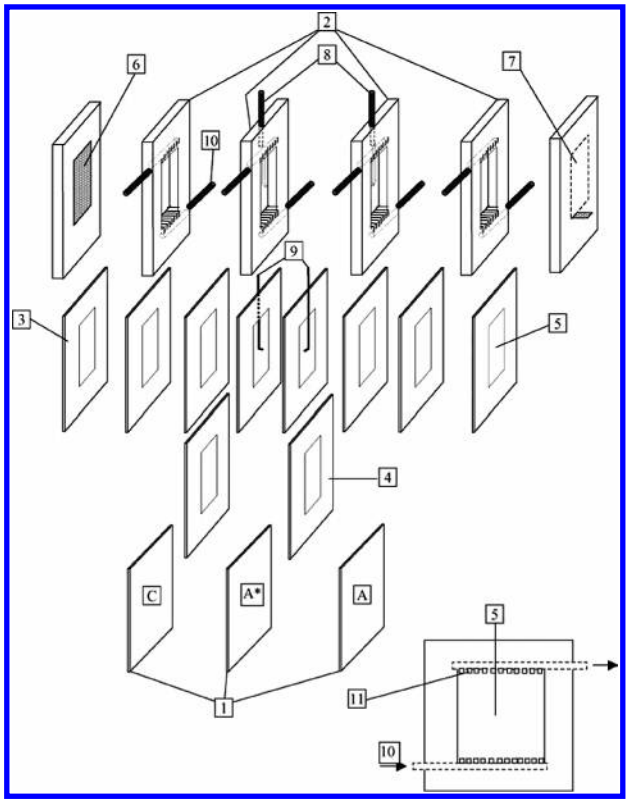

Figure 2. Diagram of the experimental cell: membranes (1); plastic gaskets (2); elastic gaskets (3,4); square aperture (5); cathode (6); anode (7); plastic capillaries (8); silver−silver chloride electrodes (9); connecting pipe (10); stream spreader of a comb shape (11); the membrane studied (A*); a cation-exchange membrane (C); an anion-exchange membrane (A).

difference, each of them is fixed at a distance of about 0.8 mm from the membrane under study. Each compartment is supplied with a solution through the connecting pipe (10) built into the plastic gaskets. Special guides for the solution in the shape of a comb (11) installed after inlet and before outlet connecting pipes provide laminar uniform flowing of solution between the membranes in the cell compartments. The latter is important to simplify the mathematical description of ion transport in the cell.

A Programmable Current Source-220, Keithley, was used to supply current through the cell, and Multimeter-3478A, Hewlett-Packard, was used as the recorder of the potential drop across the membrane under study. The Multimeter was connected to a PC equipped with special software for acquisition of CVC and ChP curves. To obtain the CVC, a current was applied with a cathode and an anode (Figure 2, positions 6 and 7), and the potential drop across the polarized membrane was measured with two silver wires (Figure 2, position 9) connected to the Multimeter.

It was established that the mass transfer in the cell presented above is well described by the convective-diffusion model[23,40] in the case where smooth homogeneous membranes are used at currents lower than the limiting one. The model supposes a laminar steady Poiseuillean flow with a parabolic velocity profile that was assured by the guides for the solution of a comb shape (Figure 2, position 11). However, this velocity distribution can be disturbed by coupled convection (a gravitational one or electroconvection) if the average velocity is small. In our experiments, the velocity was $V = 0.32$ cm s^{-1}.

According to the convective-diffusion model,[23] the limiting current density in a cell formed by ion-exchange membranes with a smooth homogeneous surface, under the condition of laminar solution flow, and in the case where the membrane length is not too great, is well approximated by eq 3 following from the Lévêque equation

$$i_{\lim} = 1.47 \frac{FDc^0}{h(T_1 - t_1)} \left(\frac{h^2 V}{LD}\right)^{1/3} \tag{3}$$

where D is the salt diffusion coefficient, c^0 the inlet concentration, h the distance between the membranes, V the average linear solution velocity, L the length of the membrane active area, T_1 and t_1 the salt counterion effective transport number in the membrane and the transport number in the solution, respectively, and F the Faraday constant. The average value of DBL can then be determined from the other known equation for the limiting current density

$$i_{\lim} = \frac{FDc^0}{\delta(T_1 - t_1)} \tag{4}$$

Results and Discussion

Current−Voltage Characteristics and pH Evolution. When comparing electrochemical behavior of different membranes by voltammetric measurements, it is convenient to use instead of the total potential drop, $\Delta\varphi_{\text{tot}}$, the quantity $\Delta\varphi'$ defined as

$$\Delta\varphi' = \Delta\varphi_{\text{tot}} - i\left(\frac{\partial\Delta\varphi_{\text{tot}}}{\partial i}\right)_{i=0} = \Delta\varphi_{\text{tot}} - iR_{\text{ef}} \tag{5}$$

where $R_{\text{ef}} = (\partial\Delta\varphi_{\text{tot}}/\partial i)_{i=0}$ is the effective resistance of the membrane system at low current densities $i \ll i_{\lim}$, which includes the ohmic resistance between the measuring electrodes and the diffusion resistance of both diffusion layers;[52] R_{ef} is determined experimentally by the initial slope of the CVC. The notion of $\Delta\varphi'$ is close to the notion of overpotential defined for electrode systems;[52,53] $\Delta\varphi'$ is named the "corrected polarization voltage" by Maletzki et al.[54] $\Delta\varphi'$ shows the excess of potential drop over the value that should take place under conservation of linear potential growth observed at $i \to 0$. The expression for $\Delta\varphi'$ is deduced in the Appendix. The use of corrected potential drop $\Delta\varphi'$ allows us to eliminate the initial ohmic resistance, which is a function of the distance between the measuring electrodes, the membrane thickness, and some other parameters that are difficult to be found, whereas they are not significant for the membrane behavior. Figure 3 presents $\Delta\varphi'$ measured through the AMX, MA-40, and MA-40-13 membranes as a function of the current density applied. The membranes were vertically or horizontally positioned, and a constant solution flow with an average velocity $V = 0.32$ cm s^{-1} was maintained in both compartments neighboring to the membrane under study. In all cases where the membrane was in horizontal position, the current was directed so that the lighter depleted layer was below the membrane under study. In this position, the depleted layer was quiescent, thus the gravitational convection was absent in the vicinity of the membrane. The gravitational convection occurred when the membrane was in the vertical position.

The shape of the obtained CVC is close to that described in numerous publications[12,15,22,27,32,36−40] and that can already be called classical. At low currents, there is a linear region (1) that transforms to a vertical straight line in coordinates $i - \Delta\varphi'$. This region is followed by an inclined plateau (region 2) replaced then by a region (3) where the slope is much higher than that of plateau. In coordinates $i - \Delta\varphi'$, the slope of region

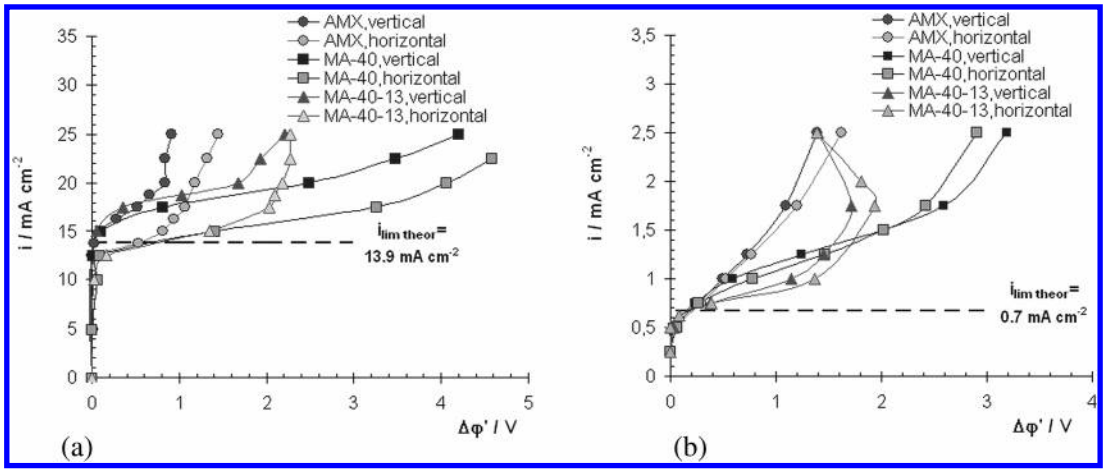

Figure 3. Current−voltage curves measured for different membranes and different positions of the cell in the Earth gravity field, under forced convection with $V = 0.32$ cm s^{-1}: (a) 0.1 M NaCl and (b) 0.005 M NaCl.

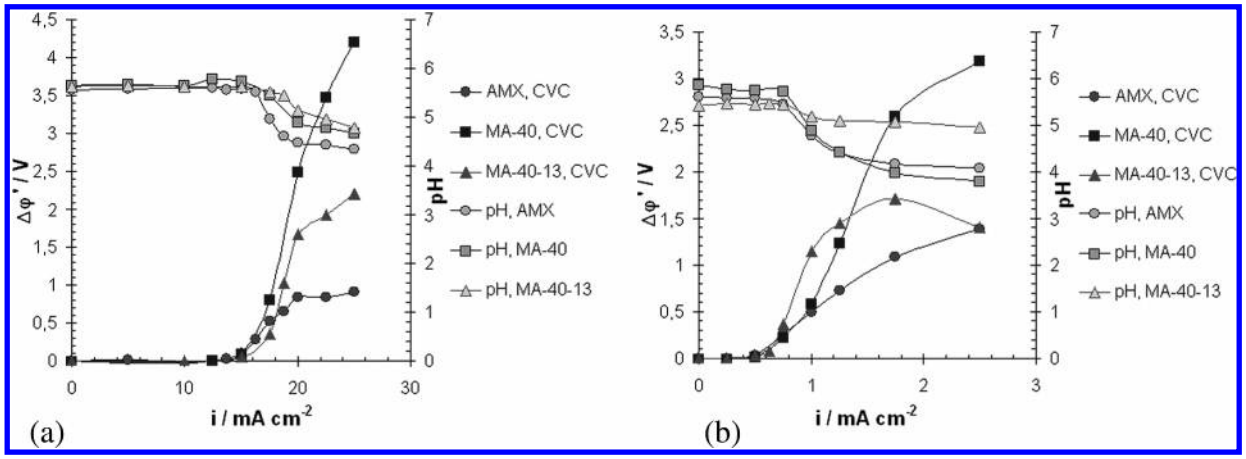

Figure 4. Current−voltage curves of vertically positioned membranes and pH evolution of the solution adjacent to the depleted membrane surface vs the current density: (a) 0.1 M NaCl and (b) 0.005 M NaCl.

3 is even negative for the MA-40-13 membrane in 0.005 M NaCl (Figure 3b). This is explained by the fact that the differential resistance of this system ($d\Delta\varphi/di$) under relatively high currents is lower than the initial resistance R.

Let us consider the CVC obtained in the horizontal position where the gravitational convection does not occur. It can be seen that the experimental value of the limiting current (found by the intersection of tangents drawn to regions 1 and 2 of CVC) is very close to the value calculated by eq 3 for both concentrations, 0.1 and 0.005 M NaCl. In calculation, the following parameters were used: $D = 1.61 \times 10^{-5}$ cm^2 s^{-1}, $T_1 = 1.000$, $t_1 = 0.604$, $V = 0.32$ cm s^{-1}, the intermembrane spacing $h = 0.7$ cm, and the membrane active area dimensions $S = 2.0 \times 2.0 = 4.0$ cm^2. The average thickness of DBL calculated from eq 4 (δ) is equal to 280 μm for these conditions.

When passing from the horizontal to the vertical position favorable for gravitational convection, a shift by 10−20% of the curve $i - \Delta\varphi'$ occurring at $i \geq i_{lim}$ in 0.1 M NaCl solution is observed. At the same time, in the case of 0.005 M solution, this passage is almost not accompanied by changes in the CVC. These observations testify that the contribution of gravitational convection is considerable in the case of the 0.1 M solution and not in 0.005 M.

It is of interest to evaluate the Rayleigh number for these two cases. In calculations, the characteristic distance d entering eq 2 is estimated as the thickness of the total DBL (δ_{tot}) at the outer edge of which the concentration $c|_{x=\delta_{tot}}$ differs from c^0 only by 1%. In the case of forced solution flowing[55] or under natural convection conditions,[56] δ_{tot} is about 1.7 times higher than δ defined above in Nernst's sense. Taking the difference in density between 0.1 M NaCl solution (outer edge of the total DBL) and pure water (at the interface under the limiting current density) as 0.004 g cm^{-3} and the characteristic length $d = \delta_{tot} = 1.7 \times 0.028 \approx 0.05$ cm, $\nu = 0.01$ cm^2 s^{-1}, and applying eq 2, one finds $Ra|_{0.1M} \approx 3000$ and $Ra|_{0.005M} \approx 150$ (where $\Delta\rho$ is assumed to be proportional to c^0). As it can be seen, the $Ra|_{0.1M}$ value is higher than the critical value (1708), whereas $Ra|_{0.005M}$ is essentially lower. Note that this evaluation does not take into account the possible heating of the interfacial solution.

As in studied membrane systems in 0.005 M solution, the gravitational convection is negligible, the overlimiting mass transfer enhancement may be assured in this case only by electroconvection and/or water splitting: by the generation of additional carriers, H^+ and OH^- ions, and the exaltation effect.

To evaluate the rate of water splitting simultaneously with registration of CVC, the pH evolution with the current density of the depleted solution adjacent to the membrane was measured with the help of a capillary adjoining to the membrane surface and through which the depleted solution flowed out (see Experimental Section) (Figure 4). As can be seen from Figure 4, pH variation begins at current density, the value of which is close for all studied membranes and which is slightly higher than the limiting one. The onset of water splitting should be related with the boundary salt concentration (c_s), which should achieve a threshold value where the H^+ (OH^-) ion concentration becomes valuable enough to ensure the transport number of this

ion to be comparable with the salt counterion transport number. This threshold may be evaluated as being of the order of 10^{-5} M, taking into account that the mobility of the H^+ (OH^-) ion is about 10 times higher than that of salt ions, with the equilibrium H^+ (OH^-) ion concentration being of the order of 10^{-7} M. In this case, the H^+ (OH^-) ion transport number should be great enough (about 10^{-1}) to provide observable changes in pH. With further increase in voltage (current density), c_s continues to decrease and the H^+ (OH^-) ion transport number is growing. However, this growth will be significant only in the case where the rate of generation of these ions at the interface is sufficiently high. The latter occurs if the membrane possesses fixed groups with high catalytic activity toward the water dissociation or if there are weak electrolytes in solution able to produce H^+ (OH^-) ions in the course of their dissociation.[8−11]

The evaluation of the polarization voltage threshold value ($\Delta\varphi'_{cr}$) at which the water splitting becomes significant may be made with eq A10 deduced in the Appendix. For $c^0 = 0.1$ M, eq A10 gives $\Delta\varphi'_{cr} = 406$ mV, while for $c^0 = 0.005$ M, $\Delta\varphi'_{cr} = 252$ mV. The experimental values for these concentrations determined for the AMX membrane are 400 ± 50 and 280 ± 20 mV, respectively.

The data presented in Figure 4 show that the replacement of weak-electrolyte secondary and tertiary amine groups within the surface layer of MA-40 membrane by strong-electrolyte quaternary amine groups results in a significant reduction of the water splitting rate: the decrease in pH of the depleted solution near the MA-40-13 membrane is noticeably less than that near the MA-40 and AMX membranes. At the same time, the increment of overlimiting current transfer is higher for the MA-40-13 membrane in comparison with the MA-40 membrane. This fact evidences the existence, at least in the case of the MA-40-13 membrane, of transfer mechanisms not related to water splitting. Generally, these mechanisms can be gravitational convection and/or electroconvection. However, the increment in overlimiting current transfer at $c^0 = 0.005$ M does not depend on the membrane position in the Earth gravity field. Hence, the gravitational convection is excluded in this case, and we can state that the main mechanism of overlimiting mass transfer, at least in the case of the MA-40-13 membrane in $c^0 = 0.005$ M NaCl solution, is electroconvection.

Note also that at an overpotential in the range of 1.5−2 V, the current density in the case of AMX (moderate water splitting rate) and MA-40-13 (low water splitting rate, the contribution of water splitting is not important) is about 4 times higher than i_{lim} in 0.005 M solution and only 1.5−2 times in 0.1 M solution. This signifies that at the same overpotential the electroconvection (which is evidently the main mechanism of overlimiting mass transfer, at least in the case of MA-40-13) increases with diluting solution. The explanation may be in the fact that the size of the SCR is larger in the case of more diluted solution, as it is follows from the theory of overlimiting transfer based on the 1D Nernst−Planck−Poisson equations.[2,23,32,36] As the maximum of space charge density is localized at the outer edge of the SCR, the further this maximum from the membrane side, the weaker the viscous resistance resulting from the nonslip condition at the membrane surface and the easier the electroconvection occurs.

The difference in intensity of electroconvection developed near the MA-40 and MA-40-13 membranes is explained by a different rate of water splitting at these membranes. When a considerable amount of H^+ ions generated in the course of water splitting is introduced into the SCR, this eliminates the electroconvection because of the Grotthus mechanism of H^+ ion transport (the case of the MA-40 membrane). The charge transfer by proton occurs across the proton channel along a chain of hydrogen bonds; the water molecules are not involved in motion. In the case of the MA-40-13 membrane, the water splitting is very low and the space charge is mainly constituted by the salt counterions (Cl^- ions), which move as rigid spheres in viscous liquid (Stokesian transport mechanism) and involve a volume of liquid in motion.

Chronopotentiograms. Analysis of chronopotentiograms can also give an insight into the problem of establishing mechanisms of overlimiting transfer. In this case, the comparison of behavior of different membranes is made by using the potential difference defined as $\Delta\varphi_{tot} - \Delta\varphi_{Ohm}$ where the ohmic potential difference $\Delta\varphi_{Ohm} = iR_{Ohm}$ is found as the jump of potential caused by current switch on, at $t = 0$. The difference between R_{Ohm} and R_{ef} defined by eq 5 is that R_{ef} includes, besides the ohmic resistance R_{Ohm}, the diffusion resistance that develops when the concentration profiles are established. Figures 5 and 6 present chronopotentiometric (ChP) curves for AMX, MA-40, and MA-40-13 membranes, obtained in 0.1 and 0.005 M NaCl solutions, respectively.

At underlimiting currents, there is no significant difference in the shape of the ChP curves obtained for different membranes both in 0.1 M and in 0.005 M NaCl solutions (Figures 5a and 6a). However, the shape of the curves is different at $i \geq i_{lim}$, which should be due to the difference in mechanisms of overlimiting current transfer acting in different membrane systems. It should be reminded that at $i \geq i_{lim}$ an inflection point appears on the initial part of ChP curve that corresponds to the so-called transition time. This time is necessary to the surface electrolyte concentration (c_s) to be decreased to a small value $c_s \ll c^0$ sufficient for starting effects of overlimiting conductance that result in restriction of the potential drop growth.

Two surface properties influence the shape of the ChP curve. The first one is the degree of surface heterogeneity, and the second one is the rate of water splitting, with the latter being a function of the ion-exchange site nature and of the surface heterogeneity. Let us consider now the factor of heterogeneity. In the case of the homogeneous AMX membrane, the slope of the initial part of the ChP curve is small, whereas the next part of the curve close to the inflection point is almost vertical (Figures 5b and 6b). In the case of MA-40 and MA-40-13 heterogeneous membranes in 0.1 M NaCl solution, the initial part of the ChP curves is more diffuse: the curves rise more sharply just after switching on the current whereas their slope near the inflection point is rather slow, in comparison with the case of AMX. The explanation[39,40] is that the surface salt concentration is distributed relatively uniformly over the AMX surface; hence, it becomes small and the limiting state is attained nearly simultaneously over all the surface that gives a sharp growth in the potential drop in the region of the inflection point. In the case of the heterogeneous membrane, the surface concentration becomes small first on the conducting regions that result in a stronger growth in the potential drop at small times lower than the transition time. Thus, the transition to the overlimiting state occurs nonsimultaneously over the surface, beginning on the conducting regions and then expanding on the neighboring nonconducting ones.

Note that in the case of the 0.005 M solution the situation changes: the initial region of the ChP curve for the MA-40-13 membrane is considerably lower than that for the MA-40 membrane and rather close to that for the AMX. This testifies that in the case of MA-40-13 there is a mechanism which prevents the interface electrolyte concentration near the conduct-

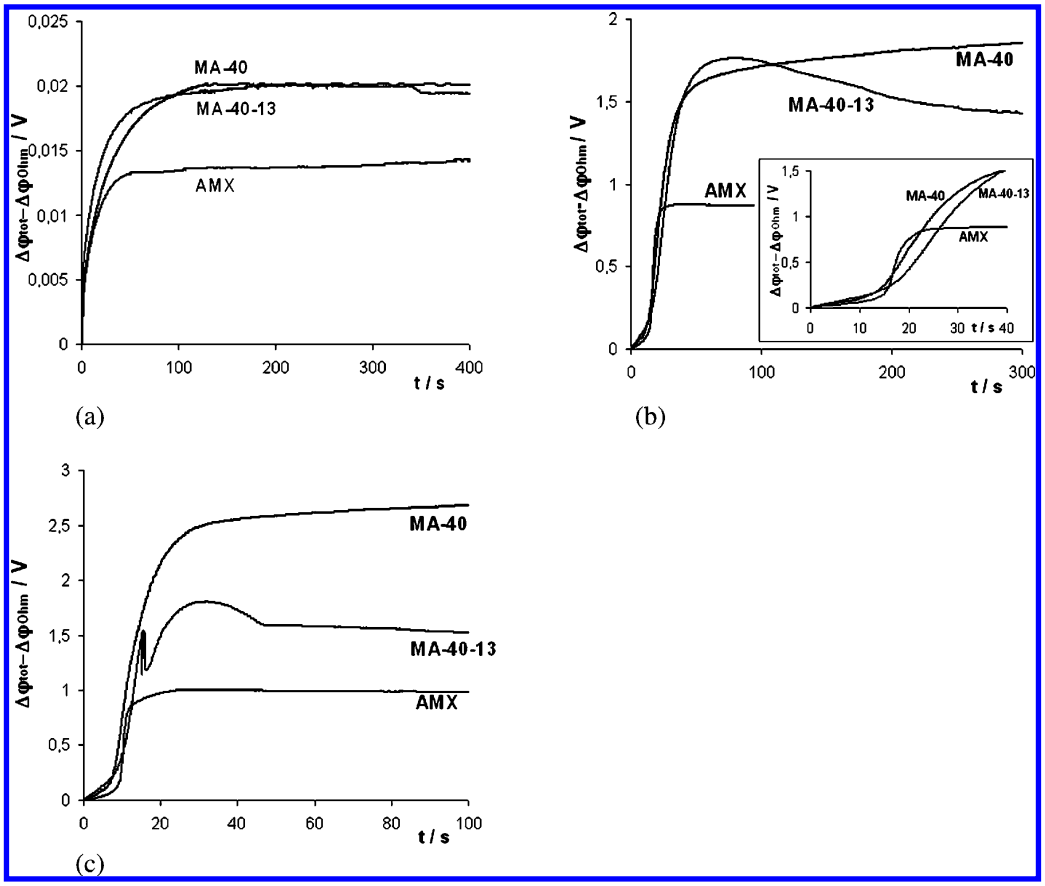

Figure 5. Chronopotentiometric curves of vertically positioned AMX, MA-40, and MA-40-13 membranes in 0.1 M NaCl solution at different current densities: (a) 5 mA cm^{-2}, (b) 20 mA cm^{-2}, and (c) 25 mA cm^{-2}.

ing regions from decrease with the same rate as in the case of MA-40. As the gravitational convection and water splitting are excluded, in the case of MA-40-13 in 0.005 M solution, this mechanism may be only the electroconvection. To explain why this phenomenon does not occur in 0.1 M solution, remember our note in the previous section that the electroconvection is more effective in more diluted solutions. To understand why the electroconvection does not develop in the case of MA-40 in 0.005 M solution, at least under relatively low potentials, consider the factor of water splitting. We have shown in the previous section that the onset of water splitting decreases with decreasing the electrolyte concentration; the threshold of the corrected potential drop is about 280 mV in 0.005 M solution. The invasion of the SCR of diluted solution near the MA-40 membrane by H^+ ions eliminates the electroconvection because of the Grotthus mechanism of H^+ ion transport, as it was explained above. The rate of water splitting at the MA-40-13 membrane is much lower; hence, the concentration of H^+ ions is too small to hinder electroconvection.

There are also considerable distinctions in the final part of ChP curves related to a quasi-stationary state. Thus, in the case of the MA-40 membrane in 0.1 M solution at $i > 17.5$ mA cm^{-2}, the potential drop continues to grow slowly for at least 10 min after the current is switched on. In the case of AMX under the same conditions, the potential drop does not change. In the case of MA-40-13, it passes through a maximum and then decreases (parts b and c of Figure 5). The behavior of the MA-40 membrane at long periods of time is caused by the generation of OH^- ions, which block gradually functional sites (secondary and tertiary amines). The specific electric conductivity of this membrane decreases dramatically when it passes into the OH^- form (Table 1) that explains the potential growth. The AMX membrane bears strong basic exchange groups, its conductivity increases when passing into the OH^- form; hence, the potential drop reaches a steady value at a relatively small time. The fact that the potential drop through the MA-40-13 membrane does not increase in a quasi-stationary state evidences once more a low rate of water splitting near its surface, as the conductivity of this membrane is low when it is in the OH^- form (Table 1). The decrease in the potential drop over this membrane at high times is perhaps caused by a gradual warming-up of the membrane and some parts of the cell and the development of gravitational convection. The fact that the potential drop does not decrease with time when the MA-40-13 is in the horizontal position, not appropriate for gravitational convection near this membrane, is in favor of this hypothesis (Figure 7a). Besides, $\Delta\varphi'$ at $t > 20$ s for MA-40-13 is higher when this membrane is in the horizontal position. Note that at $t < 20$ s the curves shown in Figure 7a are identical for both the positions; this observation evidences that the registered oscillations of potential can only be due to electroconvection.

In systems with AMX and MA-40 membranes, the effect of potential decrease with time after achieving a quasi-stationary regime is not observed perhaps because of relatively intensive water splitting occurring with the absorption of heat.

Oscillations of Potential Drop. For the MA-40-13 system at overpotentials close to 1.5 V, the potential oscillations are registered in the region of the ChP curve preceding the achievement of a maximum quasi-stationary value of $\Delta\varphi'$ (parts c and d of Figure 6). In a 0.1 M NaCl solution, several oscillations with a frequency close to 3 s^{-1} are replaced by a big wave, which turns to a slow potential decrease (without oscillations) that can be related to heating of the membrane as it was mentioned above (Figures 5c and 7a). In a 0.005 M solution,

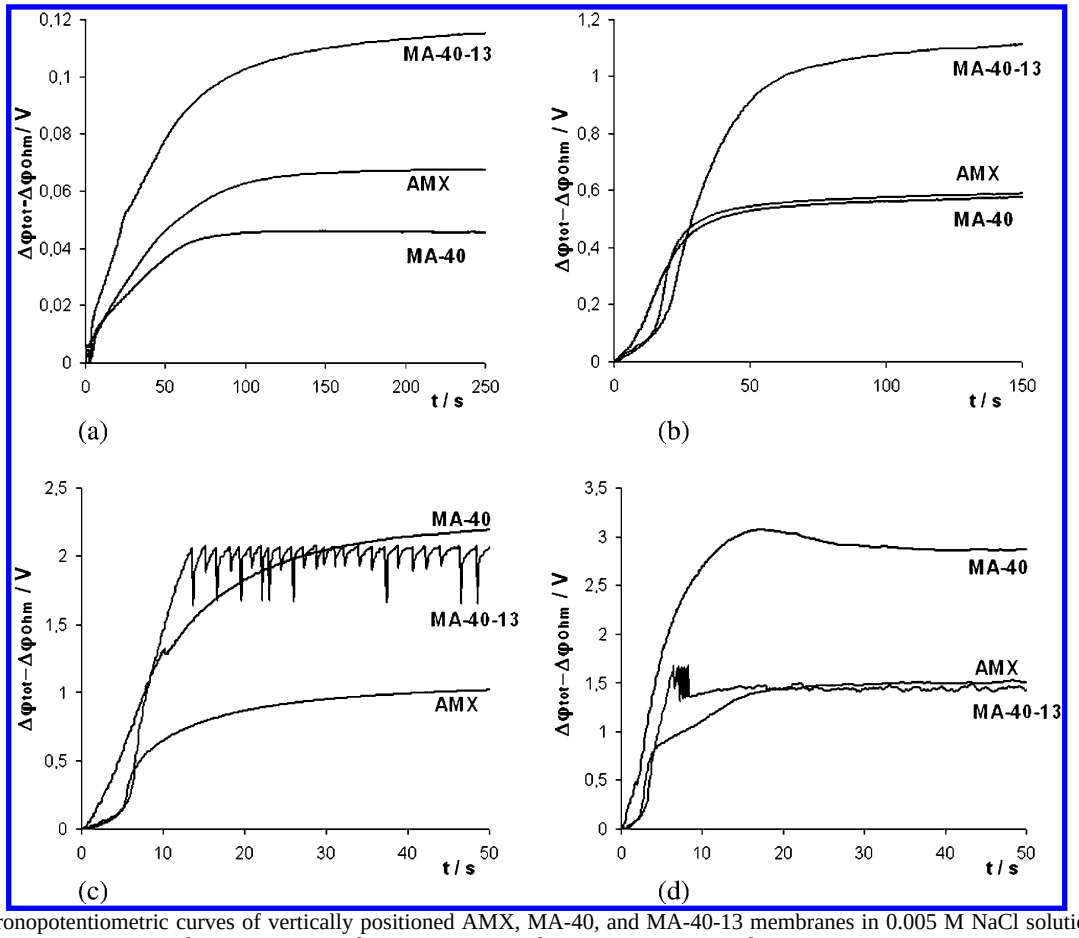

Figure 6. Chronopotentiometric curves of vertically positioned AMX, MA-40, and MA-40-13 membranes in 0.005 M NaCl solution at different current densities: (a) 0.5 mA cm^{-2}, (b) 1.0 mA cm^{-2}, (c) 1.75 mA cm^{-2}, and (d) 2.5 mA cm^{-2}.

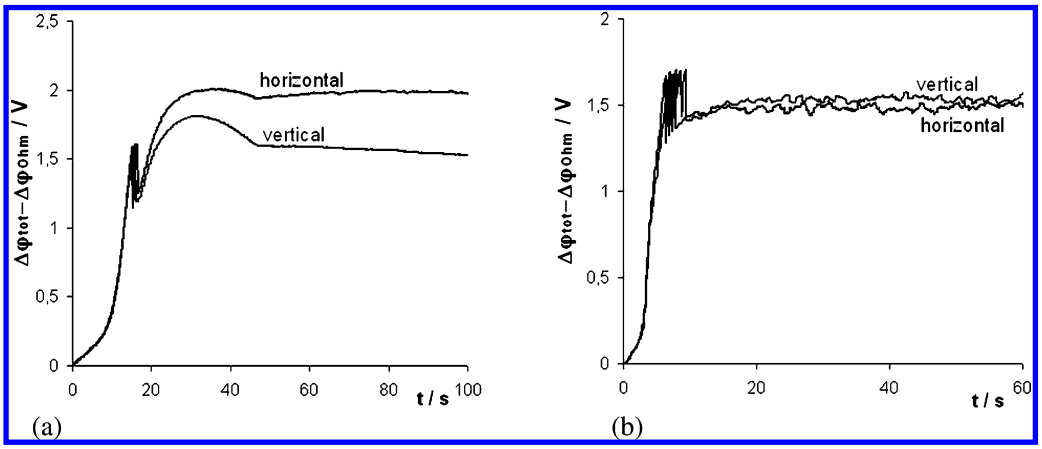

Figure 7. Potential oscillations in the MA-40-13 systems with different positions in vertical and horizontal positions: (a) 0.1 M and 25 mA cm^{-2} and (b) 0.005 M and 2.5 mA cm^{-2}.

there is a threshold of current density (about 1.5 mA cm^{-2}) and overpotential (close to 1.5 V), above which periodic oscillations appear (Figure 6c), the frequency is about 0.7 s^{-1}, and the amplitude 100 mV. At higher current densities (above 2 mA cm^{-2}), periodic oscillations are replaced, after several seconds of current passage, by chaotic ones with noticeably smaller amplitude, about 20 mV (Figure 6d). It is remarkable that the quasi-stationary corrected polarization potential drop in the MA-40-13/0.005 M NaCl system decreases with the current growth after reaching 2 V at $i = 1.75$ mA cm^{-2}; at $i =$ 2.5 mA cm^{-2}, it is equal to 1.4 V (parts c and d of Figure 6); the slope of CVC at $i > 1.75$ mA cm^{-2} is negative (Figure 3b).

Several observations may be done after analyzing the ChP and CVC curves. Independent of the concentration and the position of membrane in the Earth gravity field, the oscillations start when the corrected potential drop $\Delta\varphi'$ is in the range 1.5−2 V. After beginning the oscillations, an increase in the current density is accompanied with a relatively small and sometimes negative increment of $\Delta\varphi'$. The onset of oscillations corresponds to the beginning of the rapid current density growth following the inclined plateau of the CVC. Thus, the onset of oscillations relates to the beginning of a more intensive coupled convection increasing the mass transfer rate. The fact that the development of oscillations does not depend on the membrane position in the gravity field approves that the mechanism of oscillations is electroconvection. It is noteworthy that the electroconvection takes place as well before the onset of oscillations: it can be

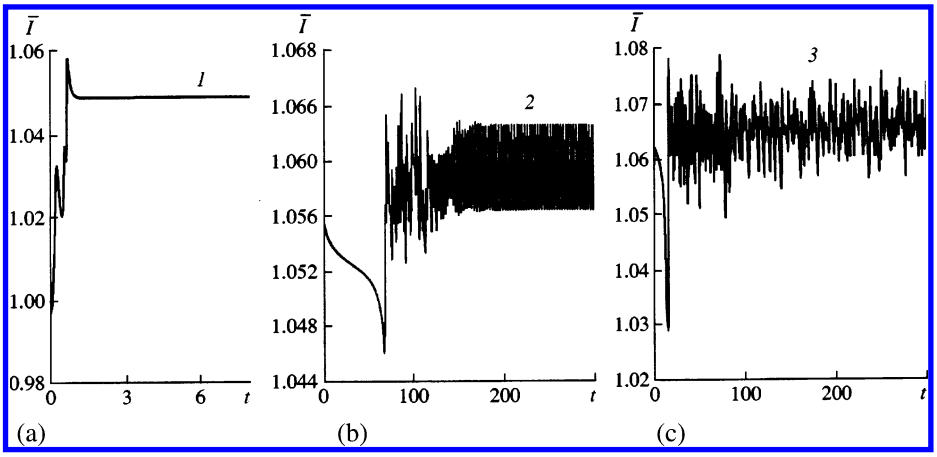

Figure 8. Time evolution of the average dimensionless current density (defined as the ratio of the current density to its limiting value) starting from a short-wave periodic disturbance:[2,32] (a) $U = \bar{U} + 1$, steady state, (b) $U = \bar{U} + 1.1$, periodic oscillations, and (c) $U = \bar{U} + 1.2$, chaotic oscillations.

seen from the growth of current density through the MA-40-13 membrane (low water splitting) above i_{lim} (Figure 3).

The scenario of the oscillation development with growing overpotential is in an excellent accordance with that predicted theoretically by Rubinstein et al.[2,32] on the basis of a model assuming that the electroconvection occurs as an electroosmotic slip of the second kind. In the case where the surface of the membrane is flat and homogeneous, the system passes from a quiescent state to a state with electroconvective mixing if the voltage exceeds a certain threshold $\bar{U}$ corresponding to the transition from stability to instability[2,32] (U is the dimensionless potential drop, normalized by $RT/F \approx 25$ mV, across the depleted diffusion layer including the quasi-equilibrium double electric layer).

If the system is in the quiescent state (the solution velocity is zero everywhere) and $U < \bar{U}$, a small perturbation of solution velocity/concentration results in diffusional damping and the system returns to the quiescent state. If $U > \bar{U}$, any small fluctuation is sufficient for initiating the process of vortices generation. Rubinstein and Zaltzman[2,32] have presented a sufficiently detailed picture of the development of hydrodynamic instability in the course of concentration polarization of a flat homogeneous permselective membrane. Along with $\bar{U}$, there is another threshold U_{cr}, depending on the membrane length $H = L/\delta$ ($U_{cr} \approx \bar{U} + 1.1$ for the "infinite" layer $H = 20$). If $\bar{U} < U < U_{cr}$, a small perturbation of velocity causes the development of paired vortices near the membrane surface, which after oscillatory readjustment in the size and shape become steady state. This process manifests itself in decaying oscillations of the electric current through the interface, with the potential drop being maintained constant (Figure 8a). Above U_{cr}, steady-state vortices become unstable. In a narrow voltage range, approximately at $U_{cr} < U < U_{cr} + 0.1$, the system approaches the state of small amplitude periodic oscillations (Figure 8b). Above this range, the oscillations become chaotic (Figure 8c). It can be seen that the presented theoretical picture conforms exactly to our experiments: compare Figures 5c, 6c, and 6d with parts a, b, and c of Figure 8, respectively.

Note that the MA-40-13 membrane is heterogeneous. For this type of membrane, Rubinstein and Zaltzman[2,32] predict a thresholdless appearance of vortex flow at low voltages. Effectively, this phenomenon may be the reason for the change in shape of the ChP curve initial region for the MA-40-13 membrane, when passing from 0.1 to 0.005 M solution: more intensive electroconvection in more diluted solution results in the lowering down of this curve from the position close to the MA-40 membrane to that of the AMX membrane (Figures 5b and 6c). However, at higher overpotentials, oscillations appear testifying hydrodynamic instability of the membrane system.

Note that intensive electroconvection is observed only in the case of the MA-40-13 membrane where low rate H^+ (OH^-) generation is produced. In the case of the MA-40 and AMX membranes, the electroconvection seems to be suppressed to a considerable degree by the water splitting.

In literature, there are a number of registrations of current/potential oscillations under polarization of ion-exchange membranes in overlimiting current regimes.[15,21−23,27,31,32,35,38,54] In particular, Maletzki et al.[54] reported that the oscillations were eliminated after immobilization of the depleted diffusion layer by a gel; the current did not rise over the plateau of limiting current density in this case. There are observations that the coupled convection is higher near cation-exchange membranes.[15,22,27] In particular, Shaposhnik et al.[26,27] have studied coupled convection by the laser interferometry technique. They found that, in a channel formed by heterogeneous membranes MA-40 and MK-40 in the vertical position, the oscillations of NaCl concentration (the inlet concentration was 0.01 M, and the distance between the neighboring membranes was 1.5 mm) developed mainly near the MK-40 cation-exchange membrane, with a frequency of about 2 s^{-1}. Near the cation-exchange membrane surface, the slope of the concentration profile is relatively high, but the amplitude of oscillations is low. The rate of water splitting was higher at the MA-40 anion-exchange membrane that followed from the fact that the pH of desalting stream solution decreased during electrodialysis.

More intensive electroconvection seems natural near cation-exchange membranes, as the Stokesian radius of cations forming the SCR near a cation-exchange membrane is usually higher than that of anions forming the SCR near an anion-exchange membrane. Besides, the water splitting, which suppresses the electroconvection, is usually more intensive near anion-exchange membranes.

Conclusions

There are four effects providing overlimiting current transfer in ion-exchange membrane systems. Two of them are related to "water splitting": the appearance of additional current carriers (H^+ and OH^- ions) and the exaltation effect increasing the salt counterion transfer. Two others are due to coupled convection partially destroying the diffusion boundary layer: gravitational free convection and electroconvection.

The exaltation effect ensures a supplement to the salt counterion flux approximately equal to 20% of the H^+ (OH^-) flux generated by water splitting. This supplement is significant if only the H^+ (OH^-) flux does exceed 50% of the total current.

The contribution of gravitational convection may be significant in membrane cells where a relatively thick diffusion boundary layer is established and at relatively high concentrations. In the cell studied here with different anion-exchange membranes, in 0.1 M NaCl solution, this effect lifts the current−voltage curve by approximately 30% while the total increment of current density over its limiting value (i_{lim}) does not exceed the value equal to i_{lim}, at corrected polarization voltages < 4 V. However, the contribution of gravitational convection decreases along with diluting solution and becomes negligible in 0.005 M NaCl solution, in the same cell. The reason is that the factors initiating this phenomenon, the concentration and temperature gradients, decrease with diluting solution.

Electroconvection makes the main contribution in overlimiting mass transfer in cells with thin DBL at low salt concentrations. It is proved in this paper by consecutive exclusion of other factors that could provide overlimiting conductance. In a 0.005 M NaCl solution, the increment of current density caused by electroconvection reaches $3i_{lim}$, under the same conditions as those in the 0.1 M solution. Experimentally observed phases of electroconvection development are in excellent agreement with those described theoretically by Rubinstein et al.[2,32] on the basis of a model assuming that the mechanism of electroconvection is nonequilibrium electroosmosis of the second kind. This agreement allows us to state that the main mechanism of overlimiting mass transfer through ion-exchange membranes in diluted solutions under high voltages is electroosmosis of the second kind, with the notion being introduced by Dukhin and Mishchuk.[19,20]

The electroconvection is highly affected by water splitting. The Stokesian radius of H^+ (OH^-) ions tends to zero: these ions carry the charge by "tunnelling" from one water molecule to another without bringing liquid volume into motion. Water splitting results in invasion of the SCR by H^+ (OH^-) ions that suppress the electroconvection.

The morphology of the membrane surface is an important factor in determining the course of ion-exchange membrane concentration polarization. On one hand, the presence of nonconducting regions on the surface results in condensation of current lines passing through well-conducting regions, which precipitates the development of current-induced effects: the decrease in surface salt concentration, the growth in potential drop, and the water splitting rate. On the other hand, nonhomogeneity of the surface hastens the onset of electroconvection. It is shown that, when the water splitting effect is eliminated, the mass transfer rate through a heterogeneous ion-exchange membrane can be higher than that through a homogeneous one, under the same polarization potential drop. This gives rise to a belief that a well-designed inhomogeneous (nonflat) membrane surface can provide a superfast mass transfer in overlimiting current regimes. Thus, the search for a relationship between membrane morphology and transport properties by structuring and modifying the surface presents one of the valuable ways for designing new membranes with improving properties.[2,57]

Acknowledgment. This work was supported by INTAS (Project No. 05-1000007-416 and No. 04-83-3878), Russian Council of President's Grants for Young Researchers (Project MK-3370.2005.3), and Russian Foundation for Basic Research (Project No. 04-03-32365) grants.

Appendix

Corrected Polarization Voltage and Evaluation of Water Splitting Threshold. The easiest way to obtain the potential drop over the diffusion boundary layer (DBL) ($\Delta\varphi_{DL}$) is through the Nernst−Planck equation describing the flux density of a salt cation (J_+). As it is the co-ion for an anion-exchange membrane considered here, J_+ is close to zero

$$J_+ = -D_+\left(\frac{dc^0}{dx} + c^0\frac{F}{RT}\frac{d\varphi}{dx}\right) = 0 \qquad (A1)$$

where c^0 is the salt concentration, which is used in view of the local electroneutrality condition assumed here: $c_+ = c_- = c^0$, an 1:1 electrolyte is considered, for the sake of simplicity; x is the normal coordinate. It follows from eq A1 that in the depleted DBL

$$\Delta\varphi_{DL}^{I} = -\frac{RT}{F}\ln\frac{c_s^I}{c^0} \qquad (A2)$$

The total potential drop between two measuring electrodes is a sum of the potential drops over depleted (denoted by superscript I) and enriched (II) DBLs, interfacial Donnan potential drops at both interfaces ($\Delta\varphi_{Don}$), and ohmic potential drops over the membrane ($\Delta\varphi_m$) and over the solution layers situated between the measuring electrodes and outer edges of the DBLs ($\Delta\varphi_{sol}$)

$$\Delta\varphi_{tot} = \Delta\varphi_{DL}^{I} + \Delta\varphi_{DL}^{II} + \Delta\varphi_{Don} + \Delta\varphi_m + \Delta\varphi_{sol} \qquad (A3)$$

Taking into account that[1]

$$\Delta\varphi_{Don} = \frac{RT}{F}\ln\frac{c_s^{II}}{c_s^{I}} \qquad (A4)$$

and applying for $\Delta\varphi_{DL}^{II}$, an equation similar to eq A1, we find

$$\Delta\varphi_{tot} = \frac{2RT}{F}\ln\frac{c_s^{II}}{c_s^{I}} + iR_{m+sol} = \frac{2RT}{F}\ln\frac{1 + i/i_{lim}}{1 - i/i_{lim}} + iR_{m+sol} \qquad (A5)$$

where R_{m+sol} is the summary ohmic resistance of the membrane and two solution layers between the measuring electrodes and outer edges of DBLs and the ratio of surface concentrations is expressed by i/i_{lim}.[1,53] Note that the overpotential (η), defined in the spirit of classical electrochemistry[52,53] as the variation of the equilibrium interfacial membrane Donnan potential drop when passing from the state with $i = 0$ to a state with nonzero current density i, will be

$$\eta = \frac{RT}{F}\ln\frac{c_s^{II}}{c_s^{I}} = \frac{RT}{F}\ln\frac{1 + i/i_{lim}}{1 - i/i_{lim}} \qquad (A6)$$

For low current densities, eq A5 can be linearized at low i/i_{lim}

$$(\Delta\varphi_{tot})_{i\to 0} = \frac{4RT}{F}\frac{i}{i_{lim}} + iR_{m+sol} \qquad (A7)$$

The effective resistance

$$R_{ef} = \left(\frac{\partial \Delta\varphi_{tot}}{\partial i}\right)_{i=0} = \frac{4RT}{Fi_{lim}} + R_{m+sol} \qquad \text{(A8)}$$

The first term in the right-hand side of eq A8 may be named the total diffusion resistance of membrane system, with each region (the depleted and enriched DBL, the depleted and enriched interfaces) giving the same contribution (equal to RT/Fi_{lim}) at $i \to 0$.

The corrected potential difference $\Delta\varphi'$ defined by eq 5 is then

$$\Delta\varphi' = \Delta\varphi_{tot} - iR_{ef} = \frac{2RT}{F}\left(\ln\frac{c_s^{II}}{c_s^{I}} - \frac{2i}{i_{lim}}\right) = \frac{2RT}{F}\left(\ln\frac{1 + i/i_{lim}}{1 - i/i_{lim}} - \frac{2i}{i_{lim}}\right) \qquad \text{(A9)}$$

The expressions in the right-hand side of eq A9 are obtained with the use of eqs A5 and A8.

Equations A5−A9 are valid at underlimiting currents when the electric space charge does not exceed the bounds of the quasi-equilibrium double layer. The comparison of calculations made with eq A10 and with a similar equation[23,36] derived when taking into account the deviation from the local electroneutrality assumption shows that the contribution of the potential drop in the SCR out of the double layer is negligible (hence, eqs A5−A9 can be applied) if $i < 0.995i_{lim}$, then the maximum value of $\Delta\varphi'$ in this case can reach 200 mV.

The threshold value of $\Delta\varphi'$, under which significant water splitting starts, can be evaluated from eq A8 when $c_s^{I} = 10^{-5}$ M, and $c_s^{II} \approx 2c^0$ while $i \approx i_{lim}$

$$\Delta\varphi'_{cr} = \frac{2RT}{F}\left(\ln\frac{2c^0}{10^{-5}} - 2\right) \qquad \text{(A10)}$$

References and Notes

(1) Helfferich, F. *Ion Exchange*; McGraw Hill: New York, 1962; p 348.
(2) Rubinstein, I.; Zaltzman, B. *Phys. Rev. E* **2000**, *62/2*, 2238.
(3) Reichmuth, D. S.; Chirica, G. S.; Kirby, B. J. *Sens. Actuators, B* **2003**, *92*, 37.
(4) Ben, Y.; Demekhin, E. A.; Chang, H.-Ch. *J. Colloid Interface Sci*. **2004**, *276*, 483.
(5) Afonso, J.-L.; Clifton, M. J. *Chem. Eng. Sci*. **2001**, *56*, 3056.
(6) Volgin, M. M.; Davydov, A. D. *Electrochim. Acta* **2004**, *49* (3), 365.
(7) Trau, M.; Saville, D. A.; Aksay, I. A. *Science* **1996**, *272*, 706.
(8) Simons, R. *Electrochim. Acta* **1984**, *29* (2), 151.
(9) Zabolotsky, V. I.; Sheldeshov, N. V.; Gnusin, N. P. *Russ. Chem. Rev*. **1988**, *57* (8), 801.
(10) Mafe, S.; Ramirez, P.; Alcaraz, A. *Chem. Phys. Lett*. **1998**, *294* (4−5), 406.
(11) Umnov, V. V.; Sheldeshov, N. V.; Zabolotsky, V. I. *Russ. J. Electrochem*. **1999**, *35* (8), 871.
(12) Forgacs, C.; Ishibashi, N.; Leibovitz, J.; Sinkovic, J.; Spiegler, K. S. *Desalination* **1972**, *10* (2), 181.
(13) Kharkats, Yu. I. *Sov. Electrochem*. **1985**, *21*, 917.
(14) Sheldeshov, N. V.; Ganych, V. V.; Zabolotsky, V. I. *Russ. J. Electrochem*. **1991**, *27* (1), 11.
(15) Zabolotsky, V. I.; Nikonenko, V. V.; Pismenskaya, N. D.; Urtenov, M. Kh.; Laktionov, E. V.; Strathmann, H.; Wessling, M.; Koops, G. H. *Sep. Purif. Technol*. **1998**, *14* (1−3), 255.
(16) Landau, L. D.; Lifshits, E. M. *Hydrodynamics*; Fizmatlit: Moscow, 2001; Vol. VI, p 731.
(17) Guyon, E.; Hulin, J.-P.; Petit, L. *Hydrodynamique physique. Matière Condensée*; Savoirs Actuels InterEditions/CNRS Editions: Paris, 2001; p 520.
(18) Volgin, V. M.; Davydov, A. D. *Russ. J. Electrochem*. **2006**, *42* (5), in press.
(19) Dukhin, S. S.; Mishchuk, N. A. *Russ. Colloid J*. **1989**, *51*, 659.
(20) Dukhin, S. *Adv. Colloid Interface Sci*. **1991**, *35*, 173.
(21) Mishchuk, N. A.; Dukhin, S. S. Electrokinetic phenomena of the second kind. In *Interfacial Electrokinetics and Electrophoresis*; Delgado, A., Ed.; Marcel Dekker: New York, 2002; p 241.
(22) Zabolotsky, V. I.; Nikonenko, V. V.; Pismenskaya, N. D. *J. Membr. Sci*. **1996**, *119* (2), 171.
(23) Zabolotsky, V. I.; Nikonenko, V. V. *Ion Transport in Membranes (in Russian)*; Nauka: Moscow, 1996; p 390.
(24) Volgin, V. M.; Volgina, O. V.; Bograchev, D. A.; Davydov, A. D. *J. Electroanal. Chem*. **2003**, *546*, 15.
(25) Pismenskiy, A. V.; Nikonenko, V. V.; Urtenov, M. Kh.; Pourcelly, G. *Desalination* **2006**, *192* (1−3), 374.
(26) Shaposhnik, V. A.; Vasil'eva, V. I.; Praslov, D. B. *J. Membr. Sci*. **1995**, *101* (1−2), 23.
(27) Shaposhnik, V. A.; Vasil'eva, V. I.; Ugryumov, R. B.; Kozhevnikov, M. S. *Russ. J. Electrochem*. **2006**, *42* (5), 531.
(28) Lifson, S.; Gavish, B.; Reich, S. *Biophys. Struct. Mech*. **1978**, *4* (1), 53.
(29) Vessler, G. P.; Krylov, V. S.; Shvarts, P.; Linder, H. *Sov. Electrochem*. **1986**, *22* (5), 623.
(30) Budnikov, E. Yu.; Maksimychev, A. V.; Kolyubin, A. V.; Timashev, S. F. *Russ. J. Electrochem*. **2001**, *37* (1), 80.
(31) Pismenskaia, N.; Sistat, Ph.; Huguet, P.; Nikonenko, V.; Pourcelly, G. *J. Membr. Sci*. **2004**, *228* (1), 65.
(32) Rubinshtein, I.; Zaltzman, B.; Pretz, I.; Linder, K. *Russ. J. Electrochem*. **2002**, *38* (8), 853.
(33) Lerman, I.; Rubinstein, I.; Zaltzman, B. *Phys. Rev. E* **2005**, *71* (1), *011506*, 1−9.
(34) Rubinstein, I.; Zaltzman, B.; Lerman, I. *Phys. Rev. E* **2005**, *72* (1), *011505*, 1−19.
(35) Mishchuk, N.; Gonzalez-Caballero, F.; Takhistov, P. *Colloids Surf., A* **2001**, *181* (1−3), 131.
(36) Urtenov, M. Kh.; Nikonenko, V. V. *Russ. J. Electrochem*. **1993**, *29* (2), 229.
(37) Choi, J.-H.; Lee, H.-J.; Moon, S.-H. *J. Colloid Interface Sci*. **2001**, *238* (1), 188.
(38) Krol, J. J.; Wessling, M.; Strathmann, H. *J. Membr. Sci*. **1999**, *162* (1−2), 155.
(39) Choi, J. H.; Kim, S. H.; Moon, S. H. *J. Colloid Interface Sci*. **2001**, *241* (1), 120.
(40) Volodina, E.; Pismenskaya, N.; Nikonenko, V.; Larchet, C.; Pourcelly, G. *J. Colloid Interface Sci*. **2005**, *285* (1), 247.
(41) Laktionov, E. V.; Nikonenko, V. V.; Pismenskaia, N. D.; Zabolotsky, V. I. *Desalination* **1996**, *108* (1−3), 149.
(42) Zabolotsky, V. I.; Nikonenko, V. V.; Pismenskaya, N. D.; Pismensky, V. F.; Lactionov, E. V. Patent 2033850 Russian Federation, MKI5 B 01 D 13/02. *Electrodialyser*. IP Membrane Technology. Krasnodar, Russia, No. 93006226; priority 04.02.93; publication 27.04.95.
(43) Eigenberger, G.; Strathmann, H.; Grabovskiy, A. Patent WO 2005/009596 A1 Germany, B01D 61/44. *Membrane assembly, electrodialysis device and method for continuous electrodialytic desalination*. Stuttgart University, Germany, No. PCT/EP2004/007961; priority 18.07.2003; publication 03.02.2005.
(44) Ibanez, R.; Stamatialis, D. F.; Wessling, M. *J. Membr. Sci*. **2004**, *239*, 119.
(45) Balavadze, E. M.; Bobreshova, O. V.; Kulintsov, P. I. *Russ. Chem. Rev*. **1988**, *57* (6), 585.
(46) Vyas, P. V.; Ray, P.; Adhikary, S. K.; Shah, B. G.; Rangarajan, R. *J. Colloid Interface Sci*. **2003**, *257* (1), 127.
(47) Nikonenko, V. V.; Pis'menskaya, N. D.; Volodina, E. I. *Russ. J. Electrochem*. **2005**, *41* (11), 1205.
(48) Berezina, N. P.; Fedorovitch, N. F.; Kononenko, N. A.; Komkova, E. N. *Russ. J. Electrochem*. **1993**, *29* (10), 1254.
(49) Berezina, N. P.; Shaposhnik, V. A.; Praslov, D. V.; Ivina, O. P. *Russ. J. Phys. Chem*. **1990**, *64*, 2790.
(50) *NEOSEPTA, Ion-exchange membranes, Catalogue*; Tokuyama Soda Co. Ltd.
(51) *Ion-Exchange Membranes. Granules. Powders, Catalogue*; Nefedova, G. Z., Klimova, Z. G., Sapozhnikova, G. S., Eds.; Moscow, 1977, in Russian.
(52) Vetter, K. J. *Electrochemical Kinetics*; Academic Press: New York, 1967; Chapter 2, pp 157−184.
(53) Manzanares, J.; Kontturi, K. Interfacial Kinetics and Mass Transport, Diffusion and Migration. In *Encyclopedia of Electrochemistry*; Bard, A. J., Stratmann, M., Calvo, E. J., Eds.; Whiley Publishing Inc.: Indianapolis, IN, 2003; Vol. 2, pp 81−121.
(54) Maletzki, F.; Rosler, H.-W.; Staude, E. *J. Membr. Sci*. **1992**, *71/1−2*, 105.
(55) Gnusin, N. P.; Zabolotsky, V. I.; Nikonenko, V. V.; Urtenov, M. Kh. *Russ. J. Electrochem*. **1986**, *22*, 298.
(56) Lerche, D.; Wolf, H. *Bioelectrochem. Bioenerg*. **1975**, *2* (4), 293.
(57) Wessling, M. Micro- and nanofabrication of membranes. *Plenary Lecture at Euromembrane 2004 Congress*; Sept 28−Oct 1, 2004, Hamburg, Germany.